



HAL
open science

Over a decade of atmospheric mercury monitoring at Amsterdam Island in the French Southern and Antarctic Lands

Olivier Magand, H el ene Angot, Yann Bertrand, Jeroen E Sonke, Laure Laffont, Sol ene Duperray, L ea Collignon, Damien Boulanger, Aur elien Dommergue

► To cite this version:

Olivier Magand, H el ene Angot, Yann Bertrand, Jeroen E Sonke, Laure Laffont, et al.. Over a decade of atmospheric mercury monitoring at Amsterdam Island in the French Southern and Antarctic Lands. *Scientific Data* , 2023, 10 (1), 10.1038/s41597-023-02740-9 . hal-04349870

HAL Id: hal-04349870

<https://hal.science/hal-04349870>

Submitted on 18 Dec 2023

HAL is a multi-disciplinary open access archive for the deposit and dissemination of scientific research documents, whether they are published or not. The documents may come from teaching and research institutions in France or abroad, or from public or private research centers.

L'archive ouverte pluridisciplinaire **HAL**, est destin ee au d ep ot et  a la diffusion de documents scientifiques de niveau recherche, publi es ou non,  emanant des  tablissements d'enseignement et de recherche fran ais ou  trangers, des laboratoires publics ou priv es.



OPEN

DATA DESCRIPTOR

Over a decade of atmospheric mercury monitoring at Amsterdam Island in the French Southern and Antarctic Lands

Olivier Magand^{1,2}, H  l  ne Angot² , Yann Bertrand², Jeroen E. Sonke³ , Laure Laffont³, Sol  ne Duperray², L  a Collignon², Damien Boulanger⁴ & Aur  lien Dommergue²

The Minamata Convention, a global and legally binding treaty that entered into force in 2017, aims to protect human health and the environment from harmful mercury (Hg) effects by reducing anthropogenic Hg emissions and environmental levels. The Conference of the Parties is to periodically evaluate the Convention's effectiveness, starting in 2023, using existing monitoring data and observed trends. Monitoring atmospheric Hg levels has been proposed as a key indicator. However, data gaps exist, especially in the Southern Hemisphere. Here, we present over a decade of atmospheric Hg monitoring data at Amsterdam Island (37.80°S, 77.55°E), in the remote southern Indian Ocean. Datasets include gaseous elemental and oxidised Hg species ambient air concentrations from either active/continuous or passive/discrete acquisition methods, and annual total Hg wet deposition fluxes. These datasets are made available to the community to support policy-making and further scientific advancements.

Background & Summary

Mercury (Hg) is a ubiquitous toxicant harmful to human health and the environment¹. This global contamination issue is addressed under the 2017 Minamata Convention (<https://www.mercuryconvention.org/en>) which commits its current 147 parties to curb anthropogenic Hg emissions to air and releases to land and water. According to Article 22 of the Convention, the Conference of the Parties (COP) is required to periodically evaluate the effectiveness of the Convention starting in 2023, and to perform this evaluation on the basis of available scientific information. The overarching goal of the effectiveness evaluation is to assess whether actions taken under the umbrella of the Minamata Convention have resulted in changes in Hg levels in the environment. Monitoring of atmospheric Hg levels and associated trend analysis has been identified as one of the primary and most appropriate tools to help evaluate the Convention's effectiveness². While Hg cycles through all environmental reservoirs, the atmosphere responds to changes in emissions much more quickly (within months) than terrestrial and oceanic reservoirs (years to decades)^{3,4}.

Hg exists in three forms in the atmosphere (Fig. 1): gaseous elemental mercury (GEM), the dominant form of atmospheric Hg, and two oxidised forms, gaseous oxidised mercury (GOM) and particulate-bound mercury (PBM). These three Hg species can be deposited to ecosystems through wet and dry processes. In the guidance report UNEP/MC/COP.4/INF/12 on monitoring Hg and Hg compounds to support the effectiveness evaluation of the Minamata Convention⁵, a three-tier approach is recommended, with a gradual increase in complexity. Tier 1 focuses on GEM and wet deposition monitoring through automated, manual, or passive sampling, and on the collection of ancillary meteorological variables. Tiers 2 and 3 involve advanced techniques for atmospheric Hg measurements (e.g., dry deposition, Hg isotope measurements) and ancillary data (e.g., carbon monoxide, ozone, particulate matter measurements). Given the analytical challenges e.g.⁶, GOM and PBM are currently not

¹Observatoire des Sciences de l'Univers    La R  union (OSU-R), UAR 3365, CNRS, Universit   de La R  union, M  t  o France, 97744, Saint-Denis, La R  union, France. ²Univ. Grenoble Alpes, CNRS, INRAE, IRD, Grenoble INP, IGE, Grenoble, France. ³G  osciences Environnement Toulouse, CNRS/IRD, Universit   Paul Sabatier Toulouse 3, Toulouse, France. ⁴CNRS, Observatoire Midi-Pyr  n  es, SEDOO, Toulouse, France. e-mail: helene.angot@univ-grenoble-alpes.fr; aurelien.dommergue@univ-grenoble-alpes.fr

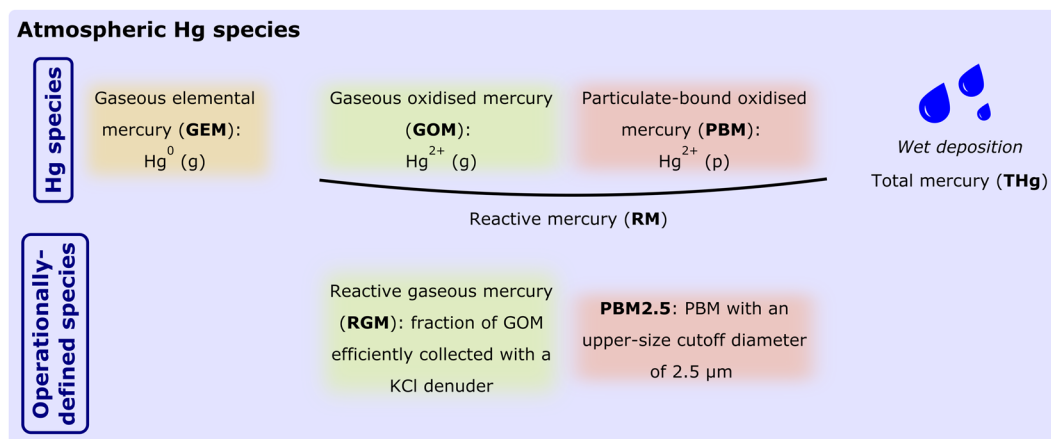


Fig. 1 Atmospheric Hg species monitored at Amsterdam Island. These acronyms are those commonly used in the Hg community and are summarised here to facilitate the reader.

recommended for monitoring in Tier 1. However, as noted in the guidance report UNEP/MC/COP.4/INF/12, “several monitoring networks and research groups perform Hg speciation measurements in a comparable manner and are encouraged to share these results, as their data will be helpful in answering questions for the effectiveness evaluation.” Further scientific work will improve understanding of biases in existing methods and comparability across measurement techniques.

Atmospheric Hg has been successfully monitored for decades through dedicated regional and global networks but with clear data gaps identified in the Southern Hemisphere^{7,8}. This issue of data coverage is particularly problematic given the natural and anthropogenic differences between hemispheres that affect the Hg biogeochemical cycle^{8,9} and, ultimately, the effectiveness evaluation. Here, we give an overview of atmospheric Hg monitoring activities carried out at Amsterdam Island (AMS; 37.80°S, 77.55°E; Fig. 2) in the southern Indian Ocean since 2012^{7,10}. Being one of the world’s most remote islands, AMS is the ideal location for monitoring the Southern Hemisphere atmospheric background. Monitoring activities have been carried out there for more than 40 years, including monitoring of greenhouse gases and other pollutants^{10–23}. The site is currently labelled global GAW/WMO (Global Atmospheric Watch/World Meteorological Organisation) and hosts monitoring activities that are part of international initiatives such as the Integrated Carbon Observation System (ICOS; <https://www.icos-cp.eu>) and, since 2012, the Global Observation System for Mercury (GOS⁴M; <http://www.gos4m.org/>)^{7,10,12,13,22}.

In an effort to support the effectiveness evaluation of the Minamata Convention, we report here Hg datasets recommended in Tier 1, i.e., ambient air GEM concentrations and total mercury (THg) wet deposition fluxes. Our datasets of oxidised Hg species (referred to as Reactive Mercury; see Fig. 1) are also being shared with the community to promote scientific progress and better understanding of the Hg cycle.

Early subsets of these observations have already been described in the literature, as detailed below: (1) For GEM active/continuous measurements, the period covered was 2012 to 2017^{7,10,12,13}, with no subsequent publication available for datasets collected from 2018 onwards. (2) For GEM passive/discrete measurements, the range was from November 2018 to November 2021²⁴, with no further description available for datasets collected since then. (3) In terms of RM active/continuous measurements, data from 2012 and 2013 were previously discussed¹⁰; however, there is no additional description of datasets collected afterwards. (4) As for RM active/discrete measurements, no description of this dataset has been presented up to the present date. (5) Lastly, wet deposition fluxes from 2013 to 2019 were published^{22,25}, without additional details provided for datasets collected from 2020 onwards.

In addition to presenting unpublished datasets collected in recent years, this data descriptor provides the first comprehensive overview of all Hg measurements performed at this site since 2012. It also offers a detailed description of all changes in instrumental setup since 2012 that may affect trend analysis, particularly in the context of the effectiveness evaluation of the Minamata Convention.

Methods

Study area. AMS is located halfway between South Africa and Australia (3200 km away from Australia, 2880 km from Reunion Island, 4200 km from South Africa, and 3300 km from the Antarctic coast) (Fig. 2). Emerging from the ocean 700 kyr before present, this small island (about 9.2 km long and 7.4 km wide; 55 km² surface area) is located at the northern margin of the southwest wind zone characterised by prevailing westerly and north-westerly winds with an average speed over 7 m/s¹¹. The island is mostly influenced by marine air masses, with occasional airflow from continental regions (Africa and South America) in the late austral winter and early spring (August to November), concomitant with the intense biomass burning season over the African continent^{10,12–14,26}.

Most of the atmospheric Hg monitoring activities described in this article are carried out at the Pointe Bénédicte observatory, located at 70 m above sea level and 2 km upwind from the main research station

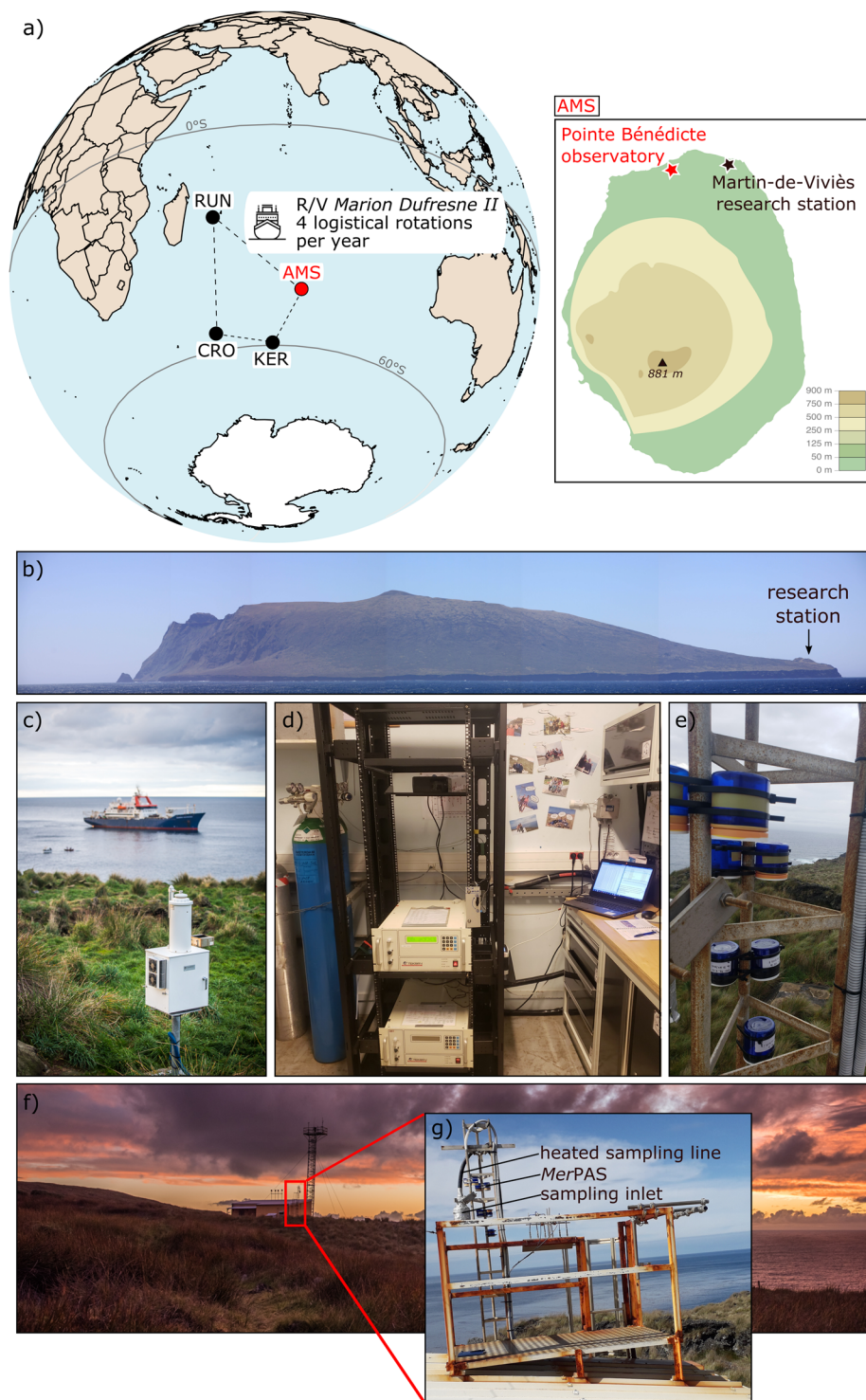


Fig. 2 Site location. (a) Location of Amsterdam Island (AMS) in the southern Indian Ocean. The island, only inhabited with approximately 20 overwintering crew members, is supplied four times a year by *RV Marion Dufresne II* (in April, August, November, and December) departing from Reunion Island (RUN). The ship also resupplies research stations located on Crozet (CRO) and Kerguelen (KER) islands, also part of the French Southern and Antarctic Lands. Most of the scientific instrumentation is located at the Pointe Bénédicte observatory, 2 km upwind from the Martin-de-Viviès main research station. (b) Panoramic view of the island. (c) Wet only collector with *RV Marion Dufresne II* in the background. (d) Interior of the Pointe Bénédicte observatory with two Tekran instruments for active/continuous measurements of GEM. (e) MerPAS systems for passive/discrete measurements of GEM. (f) Panoramic view of the Pointe Bénédicte observatory. (g) Rooftop sampling platform for atmospheric mercury measurements.

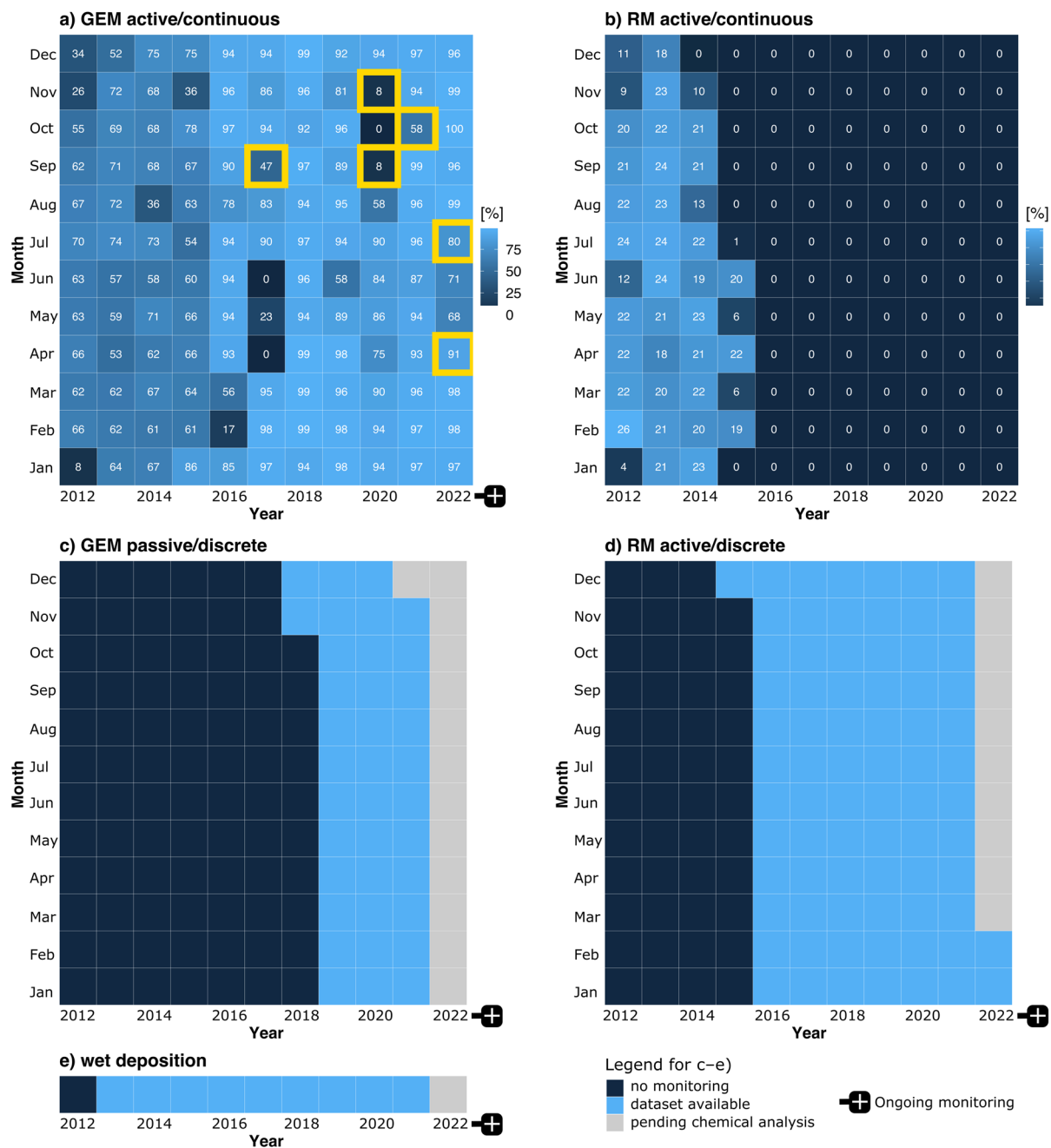


Fig. 3 Data coverage. Fraction of valid hourly measurements per month (in %) for (a) GEM and (b) RM active/continuous monitoring. That fraction is capped at 75% and 25% for GEM and RM, respectively, from Jan 2012 to Nov 2015 due to the operating principle of the Tekran[®] speciation unit. The yellow rectangles indicate when a new Tekran[®] 2537 A/B model Hg analyser was installed due to instrument failure. Panels (c–e) show current data availability for GEM passive/discrete, RM active/discrete, and wet deposition monitoring.

(Fig. 2). THg wet deposition monitoring is carried out elsewhere, at ~30 m above sea level and in the vicinity of Martin-de-Viviès.

Atmospheric Hg monitoring activities. *In situ* Hg monitoring activities are summarised in Fig. 3 and Table 1. THg wet deposition monitoring and active/continuous measurements of GEM and of the operationally-defined RGM and PBM2.5 species (Fig. 1) were initially performed under the framework of the Global Mercury Observation System (GMOS) programme (2011–2015; <https://www.gmos.eu/>; last access: 13/03/2023). The RM discrete monitoring (2015–present) is now part of the 2016–2025 GEO-flagship Global Observation System for Mercury (<https://www.earthobservations.org/>, <http://www.gos4m.org/>; last access: 13/03/2023). Passive GEM measurements (2019–present) were first done in collaboration with the research team that developed the *MerPAS* system at the University of Toronto^{27–30} and will be fully incorporated in the

Mercury species	Monitoring type	Time period	Time resolution	Sampling location	Instruments or collection system
GEM	active continuous	since Jan 2012 (ongoing)	5 min from Jan 2012 to Nov 2015; 15 min since Nov 2015	Pointe Bénédicte observatory	Cold Vapour Atomic Fluorescence Spectrometer (Tekran® 2537 A/B models)
	passive discrete	since Nov 2019 (ongoing)	Monthly to quarterly	Pointe Bénédicte observatory	Sulphur-impregnated activated carbon sorbent in Passive Air Sampler (Tekran® MerPAS)
RGM and PBM2.5	active continuous	Jan 2012 to Nov 2015	4 hours	Pointe Bénédicte observatory	Speciation unit + Cold Vapour Atomic Fluorescence Spectrometer (Tekran® 1130/1135 + 2537 A/B models)
RM	active discrete	since Nov 2015 (ongoing)	Weekly to monthly	Pointe Bénédicte observatory	Polyethersulfone Cation Exchange Membrane (Millipore®)
THg wet deposition flux	passive discrete	since Mar 2013 (ongoing)	Bi-weekly to monthly	Martin-de-Viviès research station	Automatic wet only collector (Eigenbrodt® NSA-171 model)

Table 1. List of Hg measurements performed at Amsterdam Island since 2012. See Fig. 1 for the list of acronyms and Fig. 2 for the sampling locations.

Canadian-led Global Atmospheric Passive Sampling (GAPS) network in 2024. All these monitoring activities have been implemented at AMS since 2012 within the framework of the GMOStral programme funded by the French Polar Institute.

Gaseous elemental mercury (GEM). Active measurements. A commercial Tekran® 2537 A/B model Hg analyser, commonly used at monitoring sites all over the world^{7,31,32}, has continuously been deployed at the Pointe Bénédicte observatory since January 2012^{10,12,13} (Fig. 3a). The operating principle is based on Hg enrichment on dual pure gold cartridges, followed by a thermal desorption and detection by cold vapour atomic fluorescence spectroscopy (CVAFS) ($\lambda = 253.7 \text{ nm}$)^{33,34}. Switching between two gold cartridges allows for alternating sampling and desorption modes, and results in continuous measurements. GEM was measured at a time resolution of 5 min from January 2012 to November 2015, and of 15 min since (Table 1). The integration of the signal was optimised in order to avoid potential biases and to allow comparability of the measurements regardless of the sampling frequency (5 vs 15 min), in compliance with international standards^{35,36}. This is further discussed in the **Technical Validation** section. Ambient air is sampled at 1.2 L per minute through a 10 m long heated (50 °C) and UV protected polytetrafluoroethylene (PTFE) sampling line, with an inlet installed outside at 6 m above ground level (Fig. 2f,g). From January 2012 to November 2015, the instrument was operated in speciation unit mode (see **reactive mercury species** section) ensuring that only GEM (as opposed to total gaseous mercury (TGM = GEM + GOM)) was sampled and analysed. Since the uninstallation of the speciation unit in November 2015, we have used two 0.45 μm polyethersulfone cation-exchange membranes (PES-CEM, 0.45 μm , 47 mm, Merck Millipore®) and one 0.45 μm PTFE filter (47 mm diameter), respectively installed at the inlet of the heated line and at the entrance of the instrument. This specific setup prevents any introduction of oxidised species³⁷ ensuring that, again, only GEM is sampled and analysed. The instrument is automatically calibrated every 69 h using an internal Hg permeation source which, in turn, is quarterly checked by manual injections of saturated Hg vapour collected from a temperature-controlled Tekran® 2505 Hg vapour calibration unit³⁸. The internal mass flow metre controlling the sampling flow rate is also fortnightly checked by a standardised external calibrator to prevent any drift. Concentrations are expressed in nanograms per cubic metre at standard temperature and pressure (STP; 273.15 K, 1013.25 hPa) with an instrumental detection limit below 0.1 ng/m³ and a GEM average systematic uncertainty around 10%¹². The Tekran® 2537 A/B model Hg analyser is operated according to standard operating procedures routinely applied by the Global Mercury Observation System (GMOS), the Canadian Atmospheric Mercury Measurement Network (CAMNet), and the United States Atmospheric Mercury Network (AMNet)^{7,39}.

Passive measurements. GEM has also been simultaneously measured by passive air samplers (Tekran® MerPAS) at the Pointe Bénédicte observatory since November 2019 (Fig. 3c). These passive samplers have been extensively used and tested under a wide range of climatic conditions^{27,28,40–46}, including at AMS²⁴, and have been shown to have a precision and accuracy that is comparable to that of state-of-the-art active measurement techniques²⁸. They provide an inexpensive and easy-to-use alternative to active measurements and are increasingly used worldwide. GEM is sequestered in a sulphur-impregnated activated carbon sorbent (HGR carbon, Calgon®) cartridge through a collection system using a Radiello diffusive barrier. At AMS, the MerPAS systems (samples, blanks) are deployed on a quarterly basis. They are carefully stored in well-sealed glass jars and in the dark before and after field deployment to avoid contamination and to lower blanks²⁴. Back to the laboratory, samples undergo thermal decomposition and amalgamation, and are analysed by atomic absorption spectroscopy (AMA254 (Leco® Instruments Ltd) or MA3000 (Nippon® Instruments Corporation)) using pure oxygen as carrier gas. The analytical procedure and associated metrology (calibration, blank correction, method detection and quantification limits calculation) are described in Hoang *et al.*²⁴ and McLagan *et al.*²⁹. Final volumetric air concentrations (in ng per cubic metre) are obtained by dividing the field blank-adjusted amount of Hg in each sampler (in ng) by the product of a temperature and wind-corrected sampling rate (m³/day) and the deployment duration in days²⁴.

Reactive mercury species. Continuous measurements. A commercial Tekran® 1130/1135 model speciated Hg analyser was deployed at AMS from January 2012 to November 2015 (see Fig. 3b) for the monitoring of Reactive

Mercury species	Frequency	Level	Time resolution	DOI	Reference number
GEM	active continuous	1	5/15 min	Angot, H., Dommergue, A., Magand, O. & Bertrand, Y. (2023). Continuous measurements of atmospheric mercury at Amsterdam Island (L1). [Dataset]. Aeris. https://doi.org/10.25326/345#v1.0	60
		2	1 hour	Angot, H., Dommergue, A., Magand, O. & Bertrand, Y. (2023). Continuous measurements of atmospheric mercury at Amsterdam Island (L2). [Dataset]. Aeris. https://doi.org/10.25326/168#v1.0	61
	passive discrete	1	Monthly to quarterly	Angot, H., Dommergue, A., Magand, O. & Bertrand, Y. (2023). Discrete measurements of atmospheric elemental mercury at Amsterdam Island (L1). [Dataset]. Aeris. https://doi.org/10.25326/489#v1.0	62
RGM PBM2.5	active continuous	1	4 hours	Angot, H., Dommergue, A., Magand, O. & Bertrand, Y. (2023). Continuous measurements of atmospheric mercury at Amsterdam Island (L1). [Dataset]. Aeris. https://doi.org/10.25326/345#v1.0	60
RM	active discrete	1	Weekly to monthly	Angot, H., Dommergue, A., Magand, O. & Bertrand, Y. (2023). Discrete measurements of atmospheric reactive mercury at Amsterdam Island (L1). [Dataset]. Aeris. https://doi.org/10.25326/488#v1.0	63
THg wet deposition flux	passive discrete	2	Annual	Angot, H., Dommergue, A., Magand, O. & Bertrand, Y. (2023). Total mercury wet deposition fluxes at Amsterdam Island (L2). [Dataset]. Aeris. https://doi.org/10.25326/487#v1.0	64

Table 2. Data records. Level 1 datasets represent quality-checked datasets with data in their original time resolution. Level 2 data, when available, are modified quality-checked data products (hourly mean for GEM; annual wet deposition flux). See Fig. 1 for the list of acronyms.

Mercury species	Qualification level	Variable	Definition
GEM, RGM, PBM2.5	L1	Date_time	Date and time of measurement in local time (UTC + 5; DD/MM/YYYY HH:MM:SS)
		GEM_valid	Ambient air concentration of Gaseous Elemental Mercury (GEM) in ng/m ³ at standard temperature and pressure (5–15 min time resolution)
		RGM_valid	Ambient air concentration of Reactive Gaseous Mercury (RGM) in pg/m ³ at standard temperature and pressure (4 hours time resolution)
		PBM_valid	Ambient air concentration of Particulate Bound Mercury with an upper-size cutoff diameter of 2.5 µm (PBM2.5) in pg/m ³ at standard temperature and pressure (4 hours time resolution)
GEM	L2	Date_time	Date and time of measurement in local time (UTC + 5, DD/MM/YYYY HH:MM:SS)
		GEM_valid	Hourly-averaged ambient air concentration of Gaseous Elemental Mercury (GEM) in ng/m ³ at standard temperature and pressure

Table 3. List of attributes in the files corresponding to active/continuous measurements of GEM, RGM, and PBM2.5 with a Tekran® 2537/1130/1135 Hg analyser. Note that RGM and PBM2.5 datasets are only available from 2012 to 2015.

Gaseous Mercury (RGM; a subset of GOM consisting of all forms of Hg sampled using a KCl-coated denuder⁴⁷; see Fig. 1) and Particulate Bound Mercury (PBM2.5, i.e., PBM with an upper-size cutoff diameter of 2.5 µm; see Fig. 1)^{7,10}. This so-called speciation unit system, consisting of both Tekran® 1130/1135 modules, was connected to the Tekran® 2537 A/B analyser for simultaneous GEM monitoring (see *Gaseous Elemental Mercury* section) through a 10 m long and heated (50 °C) PTFE sampling line. RGM is sequestered by the Tekran® 1130 module KCl-coated denuder while the fraction of PBM below 2.5 µm (PBM2.5; see Fig. 1) is trapped onto a quartz regenerable filter located within the Tekran® 1135 module⁴⁷. At AMS, the 1130 and 1135 modules were configured to collect RGM and PBM2.5 over a three-hour period at a 10 L/min flow rate. RGM and PBM2.5 were then sequentially thermally desorbed (500 °C for 15 min and 800 °C for 20 min, respectively) into a Hg-free air stream and subsequently analysed as GEM by the Tekran® 2537 A/B analyser. RGM and PBM2.5 concentrations are expressed in picograms per cubic metre under STP conditions with an instrumental detection limit below 0.4 and 0.3 pg/m³ for the Tekran® 1130 and 1135 modules, respectively⁴⁸. By analogy with the Tekran® 2537 A/B model, the 1130/1135 modules were operated following well established standard operating procedures³⁹.

Discrete measurements. Reactive Mercury (RM = GOM + PBM; see Fig. 1) has been collected since December 2015 (Fig. 3d) using the two PES-CEMs installed at the inlet of the Tekran® 2537 A/B model heated sampling line (see *Gaseous Elemental Mercury* section). Gustin *et al.*^{49,50} and Dunham-Cheatham *et al.*⁵¹ have shown that PES-CEMs collect RM quantitatively. Two PES-CEMs are deployed to limit RM losses due to possible breakthrough^{37,52}. Previous studies^{37,52–54} have shown the inertness of such membranes to GEM when deployed in an active sampling setting under environmental background conditions (1 to 2 ng/m³) guaranteeing no overestimation of RM and underestimation of GEM. At AMS, time-integrated RM samples are collected at a frequency ranging from ~3 to ~37 days (average ~11 days) depending on local environmental conditions.

Mercury species	Qualification level	Variable	Definition
GEM	L1	# sample	Sample identification number
		Date_time_START	Date and time of collection start in local time (UTC + 5; DD/MM/YYYY HH:MM:SS)
		Date_time_STOP	Date and time of collection finish in local time (UTC + 5; DD/MM/YYYY HH:MM:SS)
		Duration	Duration of sample collection in days
		T_avg	Average ambient air temperature in Celsius degrees during sample collection
		WS_avg	Average wind speed in m/s during sample collection
		SR_adj	Adjusted sampling rate in m ³ /day
GEM_valid	Ambient air concentration of Gaseous Elemental Mercury (GEM) in ng/m ³		

Table 4. List of attributes in the files corresponding to passive/discrete measurements of GEM with *MerPAS* samplers.

Mercury species	Qualification level	Variable	Definition
RM	L1	# sample	Sample identification number
		Date_time_START	Date and time of collection start in local time (UTC + 5; DD/MM/YYYY HH:MM:SS)
		Date_time_STOP	Date and time of collection finish in local time (UTC + 5; DD/MM/YYYY HH:MM:SS)
		Hg_mass	Mass of mercury on the sample in pg
		LOD	Analytical limit of detection in pg
		RM_valid	Ambient air Reactive Mercury (RM) concentration in pg/m ³ at standard temperature and pressure

Table 5. List of attributes in the files corresponding to active/discrete measurements of RM with polyethersulfone cation exchange membranes.

Mercury species	Qualification level	Variable	Definition
THg wet deposition flux	L2	Year	Calendar year considered
		Date_time_START	Date and time of collection start in local time (UTC + 5; DD/MM/YYYY HH:MM:SS)
		Date_time_STOP	Date and time of collection finish in local time (UTC + 5; DD/MM/YYYY HH:MM:SS)
		Total_collection_days_used	Number of collection days used for flux calculation
		Wet_dep_flux	Annual wet deposition flux in µg/m ² /year

Table 6. List of attributes in the files corresponding to THg wet deposition measurements.

This sampling frequency ensures the collection of sufficient RM mass on the membranes for further chemical analysis while limiting sampling losses. After collection, the two PES-CEMs are stored separately in Petri dishes inside double-zipper bags and kept dark frozen (−20 °C) until repatriation and chemical analysis. In the laboratory, each filter is placed in a PTFE beaker, digested in 16 mL of 2.5% inverse aqua regia and analysed with a Brooks Rand Model III CVAFS detector. The analytical procedure is further described in Maruszczak *et al.*⁵⁵ and Koenig *et al.*⁵⁶. The instrumental method detection limit is estimated to ~5 pg of Hg⁵⁶. The volume of air sampled on the membranes is extracted from the Tekran[®] 2537 A/B flow rate and RM concentration is consequently expressed in picograms per cubic metre under STP conditions.

Wet deposition fluxes. In order to estimate annual wet deposition fluxes, THg collection in precipitation has been carried out at AMS since March 2013 (Fig. 3e) following well-established international protocols²². Rain events are sampled by a commercial Eigenbrodt[®] NSA-171/KE automatic wet only collector^{22,25}. The start of a rain event induces an impulse from the infrared precipitation sensor and causes the lid to open up as follows: the lid moves up, swings to the side, and sinks down to prevent aerodynamic interference. Precipitation impacting a 100 mm borosilicate-glass funnel flows through a PTFE pipe directly into a 1 L fluorinated high density polyethylene (FLPE) sample bottle containing 0.8% v/v 30% concentrated Suprapur[®] quality hydrochloric acid. When precipitation stops, a signal from the precipitation sensor causes the collection funnel to close, ensuring that only wet fallout is collected, without interference from dry deposits. Evaporation of volatile Hg is prevented by maintaining a constant indoor temperature (below the outdoor temperature) and by using a vapour lock connected to the sampling bottle. Every single component of the sampling system is composed of chemically neutral material and is carefully cleaned with acid, following the procedure reported in Tassone *et al.*⁵⁷ and adapted from the

Tekran [®] default integration settings	<i>N-up</i> : 7	<i>N-dn</i> : 3	<i>NBase</i> : 5
	<i>V-up</i> : 5	<i>V-dn</i> : 3 LSB	<i>VBase</i> : 8 LSB
Optimised low-level integration settings	<i>N-up</i> : 6	<i>N-dn</i> : 4	<i>NBase</i> : 19
	<i>V-up</i> : 4	<i>V-dn</i> : 3 LSB	<i>VBase</i> : 1 LSB

Table 7. Tekran[®] 2537 A/B integration parameters optimisation for Hg peak detection in low-level ambient air concentration conditions. *N-up* is the number of consecutive up marks required to register an upslope condition; *V-up* is the size of each increase when Hg is detected, in analog to digital (A/D) counts (LSBs) required to be qualified as an up mark; *N-dn* is the number of consecutive down marks required to register a downslope condition; *V-dn* is the size of a decrease, also in A/D counts required to qualify as a down mark; *NBase* is the number of consecutive no changes required to register a baseline condition after a downslope has been detected and finally, *VBase* corresponds to the permissible change allowed from one reading to the next to qualify as a “no change” condition. Once *NBase* consecutive no changes have been registered, the first such reading is considered to be the end of the peak and a baseline condition is consequently flagged. LSB (Least Significant Bit) is the smallest level that an A/D can convert.

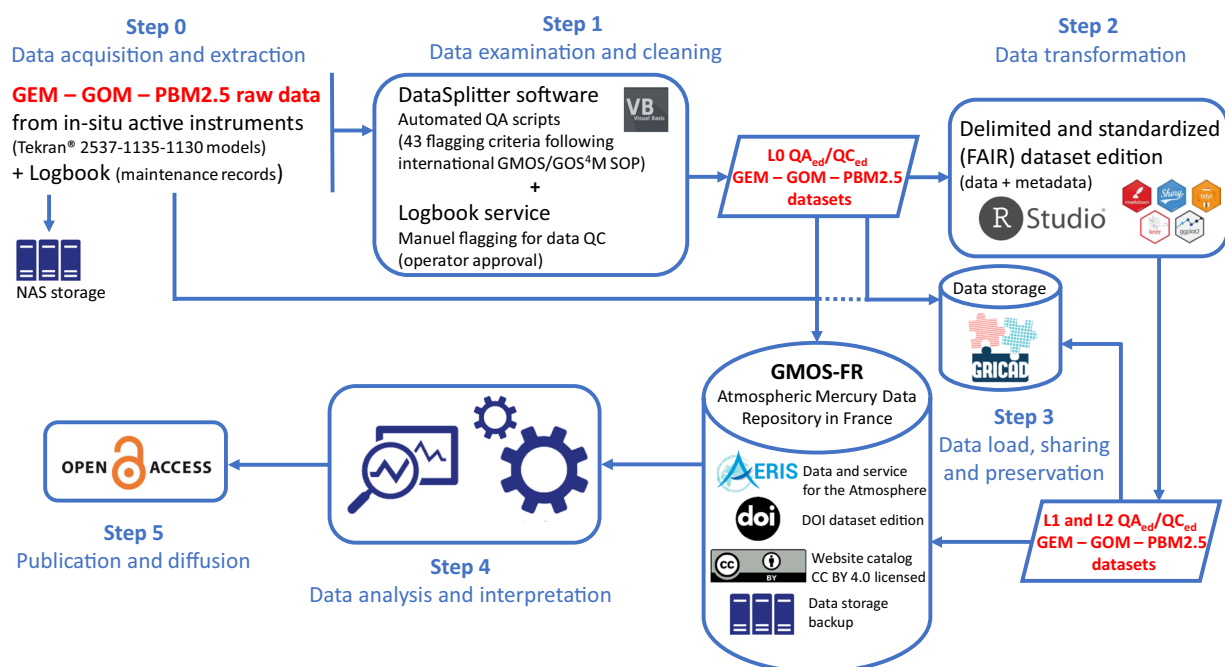


Fig. 4 Data processing workflow for GEM, GOM, and PBM2.5 active/continuous measurements (adapted from Magand *et al.*⁶⁶). Only level 1 and 2 datasets are publicly available on the GMOS-FR AERIS website.

US-EPA 1631 method⁵⁸. Integrated samples are collected over periods ranging from ~6 to ~45 days, depending on the season and on the occurrence of exceptional rainfall events, with an average fortnightly and monthly collection frequency in wet and dry periods, respectively. Precipitation samples are then kept frozen (–20 °C) and in the dark (to avoid photo-induced reduction of Hg species) until repatriation and further chemical analysis. Field, transport, bottle, and reagent blanks are also regularly collected and analysed^{25,57,59}. The complete analytical procedure and associated metrology can be found in Tassone *et al.*^{25,57}. THg values are derived according to the UNI 15853:2010 method and converted into volume-weighted mean concentration values. Annual THg wet deposition fluxes are then calculated as reported in Sprovieri *et al.*²².

Data Records

Our datasets are available under Creative Commons Attribution 4.0 International (CC-BY 4.0) Licence from the GMOS-FR AERIS website (<https://gmos.aeris-data.fr/> last access: 13/03/2023). As summarised in Table 2, level 1 and 2 data products are available on the AERIS website for active/continuous GEM measurements^{60,61}, discrete GEM measurements⁶², RGM/PBM2.5 active/continuous measurements⁶⁰, RM active measurements⁶³, and THg wet deposition fluxes⁶⁴. Tables 3–6 summarise the list of attributes for each qualified and downloadable dataset. Level 1 data represent quality-checked datasets in their original time resolution. Level 2 data, when available, are modified quality-checked data products. The GEM level 2 dataset provides hourly averaged GEM concentrations calculated from quality-controlled level 1 GEM data (5- or 15-min time resolution) when the hourly recovery rate exceeds 50% (i.e., number of valid data points vs. that possible over the reporting period). Level 2 annual THg wet deposition fluxes give the annual flux calculated based on the individual rain samples

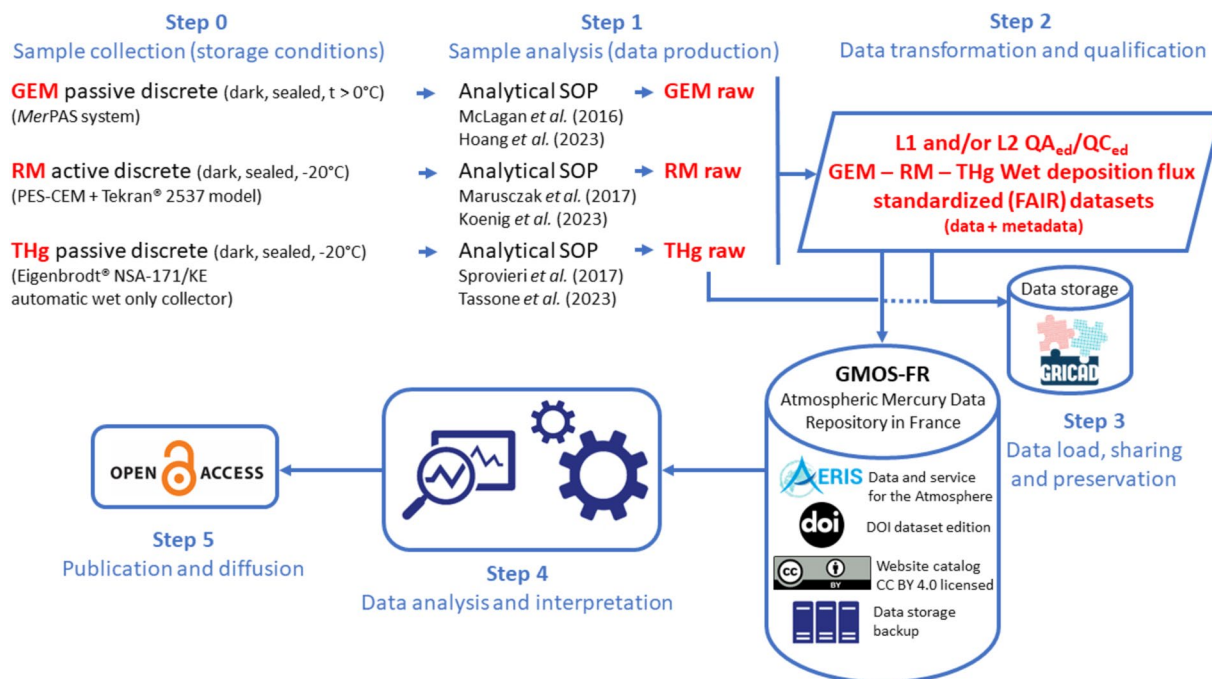


Fig. 5 Data processing workflow for discrete GEM, RM, and wet deposition measurements.

collected during the corresponding year. It is important to note that the periods considered for each annual flux do not always strictly correspond to a calendar year starting on January 1st and ending on December 31st due to logistical constraints and depending on rainfall events. Users can refer to variables 'Date_time_START' and 'Date_time_STOP' for more information (see Table 6).

Technical Validation

Active/continuous measurements of gaseous elemental mercury (GEM) and reactive mercury (RGM and PBM2.5). To ensure the comparability and the quality of the GEM/RGM/PBM2.5 active/continuous measurements, dedicated instruments and all retrieved data are respectively operated and quality controlled following established SOPs routinely applied by monitoring networks such as GMOS, CAMNet, and AMNet^{7,39} (see *Methods* section). AMS being a background air monitoring site (i.e., low atmospheric levels corresponding to $\sim 1 \text{ ng/m}^3$ or less for GEM), we have further optimised the instrumental detection capacities of the Tekran[®] 2537 A/B Hg analysers. This optimisation process, discussed with and validated by the manufacturer, guarantees the best possible sensitivity for low-level detection and quantification. More specifically, two actions were undertaken: (1) implementation of a new set of peak integration settings to improve quantification at low sample mass loading (Table 7) as discussed in Swartzendruber *et al.*³⁵, and (2) increase of the residence time in the detection cuvette by reducing the argon carrier gas flow rate to half of the manufacturer default settings while remaining within the range of recommended values (40 ml/mn and 100 ml/mn in “measure” and “flush flow” instrumental modes vs. 80 and 200 ml/mn in default settings).

Quality control procedures are applied at each step of the data processing chain, from the raw measurement to the provision of the qualified dataset. Standardised quality assurance measures and calibration tools are applied on-site to provide documented and traceable data and data products. Raw datasets as well as routine or exceptional maintenance files are compiled and processed by a custom-built software developed at the Institute of Environmental Geosciences (Grenoble, France) specifically designed for the QA/QC of the GEM/RGM/PBM2.5 datasets. In this automated process, the raw dataset is flagged (valid, warning, invalid) according to 43 possible criteria corresponding to all operation phases of the instrument (e.g., calculation of Hg concentration, calibration, sensitivity of the instrument). The inclusion of all field notes implying further invalidations (e.g., during maintenance operations) allows the production of a fully QA/QC'd dataset. Our data processing procedure is relatively close to the one developed under the umbrella of the GMOS project (G-DQM⁶⁵) but accounts for first-hand inputs from the site manager (e.g., field notes). A detailed description of this QA/QC procedure is available on the French national GMOS-FR AERIS data portal, reported in various publications^{7,10,66} and briefly summarised in Fig. 4.

It should be noted that, since 2012, we have had to replace the Tekran[®] 2537 instrument 6 times due to instrument failure or unresolved technical issues (Fig. 3a). These replacements were made following strict operating procedures (see above), with a strong focus on calibration tests, to prevent the introduction of systematic bias. Despite these occasional instrumental issues, the fraction of valid hourly measurements per month generally exceeded the 66% minimum WMO GAW requirement for continuous measurements⁶⁷ (72 out of 84 months; see Fig. 3a). From 2012–2015, this minimum requirement can be reduced to 50% given the operating

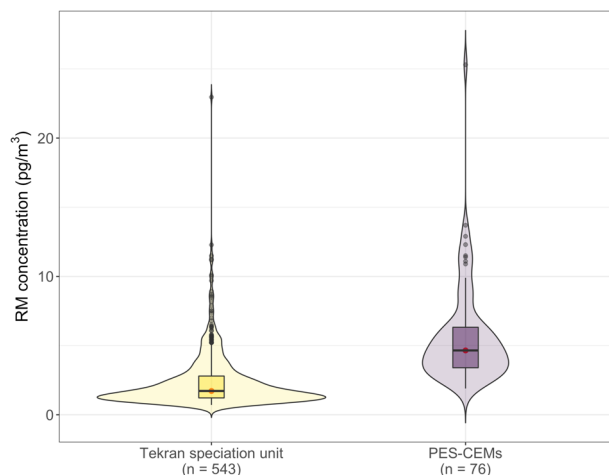


Fig. 6 Reactive Mercury (RM) concentrations inferred from the Tekran[®] speciation unit (from 2012 to 2015; RM = RGM + PBM2.5) and from the use of polyether sulfone cation-exchange membranes (PES-CEMs; from Dec 2015 to Feb 2022). *n* indicates the number of data points/samples. Note that RM measurements are still ongoing using PES-CEMs but samples collected after Feb 2022 have not been analysed yet (see Fig. 3d). The violin plots show the kernel probability density and include a marker for the median (in red) and a box indicating the interquartile range (IQR). As in standard boxplots, the upper (lower) whisker extends from the box to the largest (smallest) value no further than $1.5 \times$ IQR. Values below the detection limit were discarded.

principle of the Tekran[®] speciation unit (25% of the operating time of the 2537 analyser dedicated to RGM/PBM2.5 measurements). That target was also generally reached (43 out of 48 months; see Fig. 3a).

Discrete measurements of Gaseous elemental mercury (GEM), reactive mercury (RM), and THg wet deposition.

Figure 5 synthesises the data processing workflow related to these datasets. Operating and analytical procedures related to passive measurements of GEM with *MerPAS* systems are described in McLagan *et al.*^{27,28,30}. Additional tests were made to (1) evaluate the dependence of the passive sampling rate on meteorological conditions encountered at AMS and (2) to lower blanks. The results, reported in Hoang *et al.*²⁴, highlight the quality of our operating protocols. In addition, we follow the procedure described in McLagan *et al.*²⁹ during the subsequent chemical analysis step to prevent sulphur poisoning of catalysts.

Since 2015, RM species have been collected on two successive PES-CEMs (0.45 μm , 47 mm, Merck Millipore[®]) installed at the inlet of the Tekran[®] 2537 A/B model heated sampling line. The decision to switch from automatic and high frequency RGM/PBM2.5 measurements to discrete RM measurements was made based on the very low concentrations observed over the 2012–2015 period¹⁰ and on the need to reduce costs and power consumption. This decision was further reinforced by the growing body of literature demonstrating (1) potential sampling biases associated with the Tekran[®] speciation unit^{6,52,53,68–70} and (2) the very good performances of PES-CEMs^{50,51,55}. Depending on the speciation of oxidised Hg (e.g., HgCl₂, HgBr₂, HgO, Hg(NO₃)₂, HgSO₄), the collection efficiency of PES-CEMs is indeed 1.3 to 12 times higher than that of the Tekran[®] speciation unit^{6,50,52}. Figure 6 shows the distribution of RM concentrations observed at AMS with the Tekran[®] speciation unit (RGM + PBM2.5) and with PES-CEMs and confirms that RM concentrations inferred from the Tekran[®] speciation unit at AMS are slightly biased low by a factor of 2.7 (median (interquartile range): 1.7 (1.6) vs. 4.7 (2.9) pg/m³), in line with the literature.

Operating and analytical procedures related to the determination of the THg wet deposition flux are described in Sprovieri *et al.*²² and Tassone *et al.*²⁵ and follow the GMOS SOP adapted from the US EPA method 1631E⁵⁷. QA/QC procedures include duplicate sample analysis, precision testing using a certified reference material, matrix spikes, and regular system, transport, reagent, and field blank analysis²⁵.

Usage Notes

The standardised *.csv file format permits easy import into all analysis software commonly used in the atmospheric science community. The datasets can be used without further processing. In addition to datasets and associated metadata, the GMOS-FR AERIS website also includes a list of peer-reviewed publications that can help better understand the current state of science associated with these datasets. User should be aware that the RGM/PBM2.5 datasets collected with a Tekran[®] speciation unit may be biased, as discussed above. It is essential to consider these biases when interpreting and utilizing the data.

The data presented in this manuscript have undergone peer review in 2023 and are represented by the specific versions (#v1.0) given in Table 2. As monitoring activities are still ongoing, new datasets will be regularly uploaded to the GMOS-FR AERIS data portal. These new versions might include additional information (e.g., additional monitoring years) or refined data. Please note that any updates or new versions of the datasets are not part of the peer-reviewed data associated with this manuscript.

We welcome enquiries regarding ancillary datasets also collected at AMS by partners (e.g., meteorological conditions, greenhouse gases or ozone ambient air mole fractions) that could help interpret atmospheric Hg time-series.

Code availability

No custom code has been used during the generation of these datasets.

Received: 24 August 2023; Accepted: 9 November 2023;

Published online: 28 November 2023

References

- Basu, N. *et al.* The impact of mercury contamination on human health in the Arctic: A state of the science review. *Sci. Total Environ.* **831**, 154793 (2022).
- Evers, D. C., Keane, S. E., Basu, N. & Buck, D. Evaluating the effectiveness of the Minamata Convention on Mercury: Principles and recommendations for next steps. *Sci. Total Environ.* **569–570**, 888–903 (2016).
- Amos, H. M., Jacob, D. J., Streets, D. G. & Sunderland, E. M. Legacy impacts of all-time anthropogenic emissions on the global mercury cycle. *Glob. Biogeochem. Cycles* **27**, 410–421 (2013).
- Angot, H. *et al.* Global and Local Impacts of Delayed Mercury Mitigation Efforts. *Environ. Sci. Technol.* **52**, 12968–12977 (2018).
- Guidance on monitoring mercury and mercury compounds to support the effectiveness evaluation of the Minamata Convention | Minamata Convention on Mercury. <https://www.mercuryconvention.org/en/documents/guidance-monitoring-mercury-and-mercury-compounds-support-effectiveness-evaluation-0> (2021).
- Gustin, M. S. *et al.* Do we understand what the mercury speciation instruments are actually measuring? Results of RAMIX. *Environ. Sci. Technol.* **47**, 7295–7306 (2013).
- Sprovieri, F. *et al.* Atmospheric mercury concentrations observed at ground-based monitoring sites globally distributed in the framework of the GMOS network. *Atmos Chem Phys* **16**, 11915–11935 (2016).
- Schneider, L. *et al.* A synthesis of mercury research in the Southern Hemisphere, part 1: Natural processes. *Ambio* <https://doi.org/10.1007/s13280-023-01832-5> (2023).
- Fisher, J. A. *et al.* A synthesis of mercury research in the Southern Hemisphere, part 2: Anthropogenic perturbations. *Ambio* <https://doi.org/10.1007/s13280-023-01840-5> (2023).
- Angot, H., Barret, M., Magand, O., Ramonet, M. & Dommergue, A. A 2-year record of atmospheric mercury species at a background Southern Hemisphere station on Amsterdam Island. *Atmos Chem Phys* **14**, 11461–11473 (2014).
- Baboukas, E., Sciare, J. & Mihalopoulos, N. Spatial, Temporal and Interannual Variability of Methanesulfonate and Non-Sea-Salt Sulfate in Rainwater in the Southern Indian Ocean (Amsterdam, Crozet and Kerguelen Islands). *J. Atmospheric Chem.* **48**, 35–57 (2004).
- Slemr, F. *et al.* Comparison of mercury concentrations measured at several sites in the Southern Hemisphere. *Atmos Chem Phys* **15**, 3125–3133 (2015).
- Slemr, F. *et al.* Atmospheric mercury in the Southern Hemisphere – Part 1: Trend and inter-annual variations in atmospheric mercury at Cape Point, South Africa, in 2007–2017, and on Amsterdam Island in 2012–2017. *Atmospheric Chem. Phys.* **20**, 7683–7692 (2020).
- Li, C. *et al.* A peat core Hg stable isotope reconstruction of Holocene atmospheric Hg deposition at Amsterdam Island (37.8oS). *Geochim. Cosmochim. Acta* <https://doi.org/10.1016/j.gca.2022.11.024> (2022).
- Gaudry, A., Ascencio, J. M. & Lambert, G. Preliminary study of CO₂ variations at Amsterdam Island (Territoire des Terres Australes et Antarctiques Françaises.). *J. Geophys. Res. Oceans* **88**, 1323–1329 (1983).
- Gros, V., Poisson, N., Martin, D., Kanakidou, M. & Bonsang, B. Observations and modeling of the seasonal variation of surface ozone at Amsterdam Island: 1994–1996. *J. Geophys. Res.* **103**, 28,103–109 (1998).
- Gros, V., Bonsang, B., Martin, D. & Novelli, P. C. Carbon monoxide short term measurements at Amsterdam Island: estimation of biomass burning rates. *Chemosphere Glob. Change Sci* **1**, 163–172 (1999).
- Sciare, J., Baboukas, E., Hancy, R., Mihalopoulos, N. & Nguyen, B. C. Seasonal Variation of Dimethylsulfoxide in Rainwater at Amsterdam Island in the Southern Indian Ocean: Implications on the Biogenic Sulfur Cycle. *J. Atmospheric Chem.* **30**, 229–240 (1998).
- Sciare, J., Kanakidou, M. & Mihalopoulos, N. Diurnal and seasonal variation of atmospheric dimethylsulfoxide at Amsterdam Island in the southern Indian Ocean. *J. Geophys. Res. Atmospheres* **105**, 17257–17265 (2000).
- Sciare, J., Mihalopoulos, N. & Baboukas, E. Short-term variations of dimethylsulfide and its oxidation products at Amsterdam Island during summer time. *J. Atmospheric Chem.* **39**, 281–302 (2001).
- Sciare, J. *et al.* Long-term observations of carbonaceous aerosols in the austral ocean atmosphere: evidence of a biogenic marine organic source. *J. Geophys. Res.* **114**, D15302 (2009).
- Sprovieri, F. *et al.* Five-year records of mercury wet deposition flux at GMOS sites in the Northern and Southern hemispheres. *Atmos Chem Phys* **17**, 2689–2708 (2017).
- El Yazidi, A. *et al.* Identification of spikes associated with local sources in continuous time series of atmospheric CO, CO₂ and CH₄. *Atmospheric Meas. Tech.* **11**, 1599–1614 (2018).
- Hoang, C. *et al.* Probing the limits of sampling gaseous elemental mercury passively in the remote atmosphere. *Environ. Sci. Atmospheres* <https://doi.org/10.1039/D2EA00119E> (2023).
- Tassone, A. *et al.* Seven-year monitoring of mercury in wet precipitation and atmosphere at the Amsterdam Island GMOS station. *Heliyon* **9**(3), e14608 (2023).
- Moody, J. L. *et al.* Precipitation composition and its variability in the southern indian ocean: amsterdam island, 1980–1987. *J. Geophys. Res.* **96**, 20,769–20,786 (1991).
- McLagan, D. S. *et al.* A High-Precision Passive Air Sampler for Gaseous Mercury. *Environ. Sci. Technol. Lett.* **3**, 24–29 (2016).
- McLagan, D. *et al.* Global evaluation and calibration of a passive air sampler for gaseous mercury. *Atmospheric Chem. Phys.* **18**, 5905–5919 (2018).
- McLagan, D. S., Huang, H., Lei, Y. D., Wania, F. & Mitchell, C. P. J. Application of sodium carbonate prevents sulphur poisoning of catalysts in automated total mercury analysis. *Spectrochim. Acta Part B At. Spectrosc.* **133**, 60–62 (2017).
- McLagan, D. S., Mazur, M. E. E., Mitchell, C. P. J. & Wania, F. Passive air sampling of gaseous elemental mercury: a critical review. *Atmospheric Chem. Phys.* **16**, 3061–3076 (2016).
- Angot, H. *et al.* Chemical cycling and deposition of atmospheric mercury in polar regions: review of recent measurements and comparison with models. *Atmospheric Chem. Phys.* **16**, 10735–10763 (2016).
- Gay, D. A. *et al.* The Atmospheric Mercury Network: measurement and initial examination of an ongoing atmospheric mercury record across North America. *Atmos Chem Phys* **13**, 11339–11349 (2013).
- Fitzgerald, W. F. & Gill, G. A. Subnanogram determination of mercury by two-stage gold amalgamation and gas detection applied to atmospheric analysis. *Anal. Chem.* **51**, 1714–1720 (1979).
- Bloom, N. S. & Fitzgerald, W. F. Determination of volatile mercury species at the picogram level by low temperature gas chromatography with cold-vapor atomic fluorescence detection. *Anal. Chim. Acta* **208**, 151–161 (1988).

35. Swartzendruber, P. C., Jaffe, D. A. & Finley, B. Improved fluorescence peak integration in the Tekran 2537 for applications with sub-optimal sample loadings. *Atmos. Environ.* **43**, 3648–3651 (2009).
36. Ambrose, J. L. Improved methods for signal processing in measurements of mercury by Tekran[®] 2537A and 2537B instruments. *Atmos Meas Tech* **10**, 5063–5073 (2017).
37. Miller, M. B., Dunham-Cheatham, S. M., Gustin, M. S. & Edwards, G. C. Evaluation of cation exchange membrane performance under exposure to high Hg⁰ and HgBr₂ concentrations. *Atmospheric Meas. Tech.* **12**, 1207–1217 (2019).
38. Dumarey, R., Temmerman, E., Dams, R. & Hoste, J. The accuracy of the vapour injection calibration method for the determination of mercury by amalgamation/cold vapour atomic spectrometry. *Anal. Chim. Acta* **170**, 337–340 (1985).
39. Steffen, A., Scherz, T., Oslon, M., Gay, D. A. & Blanchard, P. A comparison of data quality control protocols for atmospheric mercury speciation measurements. *J. Environ. Monit.* **14**, 752–765 (2012).
40. McLagan, D. S. *et al.* The effects of meteorological parameters and diffusive barrier reuse on the sampling rate of a passive air sampler for gaseous mercury. *Atmospheric Meas. Tech.* **10**, 3651–3660 (2017).
41. McLagan, D. *et al.* Identifying and evaluating urban mercury emission sources through passive sampler-based mapping of atmospheric concentrations. *Environ. Res. Lett.* **13**, 074008 (2018).
42. McLagan, D. S. *et al.* Characterization and Quantification of Atmospheric Mercury Sources Using Passive Air Samplers. *J. Geophys. Res. Atmospheres* **124**, 2351–2362 (2019).
43. McLagan, D. S., Osterwalder, S. & Biester, H. Temporal and spatial assessment of gaseous elemental mercury concentrations and emissions at contaminated sites using active and passive measurements. *Environ. Res. Commun.* **3**, 051004 (2021).
44. Wohlgenuth, L., McLagan, D., Flückiger, B., Vienneau, D. & Osterwalder, S. Concurrently Measured Concentrations of Atmospheric Mercury in Indoor (household) and Outdoor Air of Basel, Switzerland. *Environ. Sci. Technol. Lett.* **7**, 234–239 (2020).
45. Si, M. *et al.* Measurement of atmospheric mercury over volcanic and fumarolic regions on the north island of New Zealand using passive air samplers. *ACS Earth Space Chem.* **4**(12), 2435–2443, <https://doi.org/10.1021/acsearthspacechem.0c00274.s001> (2020).
46. Naccarato, A. *et al.* A field intercomparison of three passive air samplers for gaseous mercury in ambient air. *Atmospheric Meas. Tech.* **14**, 3657–3672 (2021).
47. Landis, M. S., Stevens, R. K., Schaedlich, F. & Prestbo, E. M. Development and Characterization of an Annular Denuder Methodology for the Measurement of Divalent Inorganic Reactive Gaseous Mercury in Ambient Air. *Environ. Sci. Technol.* **36**, 3000–3009 (2002).
48. Wang, F. *et al.* Enhanced production of oxidised mercury over the tropical Pacific Ocean: a key missing oxidation pathway. *Atmospheric Chem. Phys.* **14**, 1323–1335 (2014).
49. Gustin, M. S., Amos, H. M., Huang, J., Miller, M. B. & Heidecorn, K. Measuring and modeling mercury in the atmosphere: a critical review. *Atmos Chem Phys* **15**, 5697–5713 (2015).
50. Gustin, M. S., Dunham-Cheatham, S. M., Huang, J., Lindberg, S. & Lyman, S. N. Development of an Understanding of Reactive Mercury in Ambient Air: A Review. *Atmosphere* **12**, 73 (2021).
51. Dunham-Cheatham, S. M., Lyman, S. & Gustin, M. S. Evaluation of sorption surface materials for reactive mercury compounds. *Atmos. Environ.* **242**, 117836 (2020).
52. Huang, J., Miller, M. B., Weiss-Penzias, P. & Gustin, M. S. Comparison of Gaseous Oxidized Hg Measured by KCl-Coated Denuders, and Nylon and Cation Exchange Membranes. *Environ. Sci. Technol.* **47**, 7307–7316 (2013).
53. Huang, J. & Gustin, M. S. Uncertainties of gaseous oxidized mercury measurements using KCl-coated denuders, cation-exchange membranes, and nylon membranes: humidity influences. *Environ. Sci. Technol.* **49**(10), 6102–6108 (2015).
54. Lyman, S. *et al.* Automated Calibration of Atmospheric Oxidized Mercury Measurements. *Environ. Sci. Technol.* **50**, 12921–12927 (2016).
55. Maruszczak, N., Sonke, J. E., Fu, X. & Jiskra, M. Tropospheric GOM at the Pic du Midi Observatory—Correcting Bias in Denuder Based Observations. *Environ. Sci. Technol.* **51**(2), 863–869, <https://doi.org/10.1021/acs.est.6b04999> (2017).
56. Koenig, A. M. *et al.* Mercury in the free troposphere and bidirectional atmosphere–vegetation exchanges – insights from Maïdo mountain observatory in the Southern Hemisphere tropics. *Atmospheric Chem. Phys.* **23**, 1309–1328 (2023).
57. Tassone, A. *et al.* Modification of the EPA method 1631E for the quantification of total mercury in natural waters. *MethodsX* **7**, 100987 (2020).
58. United States Environment Protection Agency, *Method 1631, Revision E: Mercury in water by oxidation, purge and trap, and cold vapor atomic fluorescence spectrometry*. Report No. EPA-821-R-02-019 (2002).
59. Munthe, J., Sprovieri, F., Horvat, M. & Ebinghaus, R. SOPs and QA/QC protocols regarding measurements of TGM, GEM, RGM, TPM and mercury in precipitation in cooperation with WP3, WP4 and WP5. GMOS deliverable 6.1, CNR-IIA, IVL. <http://www.gmos.eu>, last access: 3 March 2014. (2011).
60. Angot, H., Dommergue, A., Magand, O. & Bertrand, Y. Continuous measurements of atmospheric mercury at Amsterdam Island (L1). *AERIS* <https://doi.org/10.25326/345#v1.0> (2023).
61. Angot, H., Dommergue, A., Magand, O. & Bertrand, Y. Continuous measurements of atmospheric mercury at Amsterdam Island (L2). *AERIS* <https://doi.org/10.25326/168#v1.0> (2023).
62. Angot, H., Dommergue, A., Magand, O. & Bertrand, Y. Discrete measurements of atmospheric elemental mercury at Amsterdam Island (L1). *AERIS* <https://doi.org/10.25326/489#v1.0> (2023).
63. Angot, H., Dommergue, A., Magand, O. & Bertrand, Y. Discrete measurements of atmospheric reactive mercury at Amsterdam Island (L1). *AERIS* <https://doi.org/10.25326/488#v1.0> (2023).
64. Angot, H., Dommergue, A., Magand, O. & Bertrand, Y. Total mercury wet deposition fluxes at Amsterdam Island (L2). *AERIS* <https://doi.org/10.25326/487#v1.0> (2023).
65. D'Amore, F., Bencardino, M., Cinnirella, S., Sprovieri, F. & Pirrone, N. Data quality through a web-based QA/QC system: implementation for atmospheric mercury data from the global mercury observation system. *Environ. Sci. Process. Impacts* **17**, 1482–1491 (2015).
66. Magand, O., Boulanger, D. & Dommergue, A. GMOS-FR (Global Mercury Observation System – FRance) Research Data Management Plan for Atmospheric Mercury datasets. *Zenodo*, <https://doi.org/10.5281/zenodo.7406251> (2022).
67. Global Atmospheric Watch. *Guidelines for continuous measurements of ozone in the troposphere*. 82 https://library.wmo.int/doc_num.php?explnum_id=7814 (2013).
68. Lyman, S. N., Jaffe, D. A. & Gustin, M. S. Release of mercury halides from KCl denuders in the presence of ozone. *Atmospheric Chem. Phys.* **10**, 8197–8204 (2010).
69. Ambrose, J., Lyman, S., Huang, J., Gustin, M. S. & Jaffe, D. A. Fast time resolution oxidized mercury measurements during the Reno atmospheric mercury intercomparison experiment (RAMIX). *Environ. Sci. Technol.* **47**, 7285–7294 (2013).
70. Jaffe, D. A. *et al.* Progress on understanding atmospheric mercury hampered by uncertain measurements. *Environ. Sci. Technol.* **48**, 7204–7206 (2014).

Acknowledgements

We deeply thank the overwintering staff for their tremendous work (Boris Bouillard and Erwan Coz in 2012, Matthieu Le Dréau and Alice Croguennoc in 2013, Vincent Lucaire and Jeffrey Chastaing in 2014, Joyce Marais and Nicolas Joly in 2015, Isabelle Jouvie in 2016, Marine de Florinier in 2017, Yann Bertrand in 2018, Elisabeth Logeais in 2019, Laura Noël in 2020, Sophia Laporte in 2021, Solène Duperray in 2022, and Virgile

Legendre in 2023), Manuel Barret for his help with the initial setup, the French Polar Institute Paul-Emile Victor (IPEV) (<https://institut-polaire.fr/>) and Terres Australes et Antarctique Françaises (TAAF) (<https://taaf.fr/>) technical teams who contributed to the setup and maintenance of our Hg instruments under the framework of the GMOSTral-1028 IPEV program and made this endeavour possible. We also warmly thank our national and international partners and colleagues who contributed to this effort: Antonella Tassone, Attilio Naccarato, Francesca Sprovieri, and Nicola Pirrone (IIA-CNR, Italy) for the analysis of THg in precipitation samples, Frank Wania, Ying Duan, and Christopher Hoang (University of Toronto, Canada) for the analysis of *MerPAS* samples, as well as Stefan Osterwalder, Beatriz F. Arraujo, and Alkuin Koenig for their help with the chemical analysis of PES-CEMs. We would also like to thank the French national centre for Atmospheric data and services AERIS (<https://www.aeris-data.fr/>) for the maintenance of the GMOS-FR data portal. Our monitoring activities at Amsterdam Island were made possible thanks to the financial support of the European Union 7th Framework Programme project Global Mercury Observation System (GMOS 2010–2015 Nr. 26511), the French Polar Institute IPEV via the GMOSTral-1028 IPEV programme since 2012, the LEFE CHAT CNRS/INSU, and the H2020 ERA-PLANET (Nr. 689443) iGOSP programme.

Author contributions

A.D. and O.M. initiated the long-term monitoring effort at Amsterdam Island and secured funding over the years. Y.B., O.M. and H.A. led the *in situ* monitoring activities and performed the annual on-site visits for maintenance operations. O.M., Y.B. and H.A. performed the data processing. L.L., S.D., L.C., J.E.S. and O.M. conducted RM analysis and associated data treatment for discrete samples. D.B. managed the GMOS-FR AERIS platform. O.M. and H.A. wrote the manuscript with contributions from all co-authors.

Competing interests

The authors declare no competing interests.

Additional information

Correspondence and requests for materials should be addressed to H.A. or A.D.

Reprints and permissions information is available at www.nature.com/reprints.

Publisher's note Springer Nature remains neutral with regard to jurisdictional claims in published maps and institutional affiliations.



Open Access This article is licensed under a Creative Commons Attribution 4.0 International License, which permits use, sharing, adaptation, distribution and reproduction in any medium or format, as long as you give appropriate credit to the original author(s) and the source, provide a link to the Creative Commons licence, and indicate if changes were made. The images or other third party material in this article are included in the article's Creative Commons licence, unless indicated otherwise in a credit line to the material. If material is not included in the article's Creative Commons licence and your intended use is not permitted by statutory regulation or exceeds the permitted use, you will need to obtain permission directly from the copyright holder. To view a copy of this licence, visit <http://creativecommons.org/licenses/by/4.0/>.

© The Author(s) 2023